DEVELOPEMENT OF VIBRODIAGNOSTIC SYSTEM OF TRAM WHEEL FOR DAMAGE ANALYSIS

Luděk Pešek, František Vaněk, Miroslav Balda, Pavel Procházka
Petr Vaněk, Jan Cibulka, Vítězslav Bula*

The vibrodiagnostic system VDS-UT2 was developed for the investigation of a tram wheel operational vibration and deformation. The system consists of measuring, acquisition and processing tools for monitoring of tram wheels and their operational parameters, e.g. static and dynamic deformation, displacement, velocity, acceleration and temperature. The measuring on a rotating wheel is realized both by telemetric and by top-timing system. Measured data can be remote-observed via Internet connection with the control PC. The acquisition system by Starmans Electronics s.r.o. provides continuous analog and digital data logging. The control PC processes digital logical signals and evaluates time intervals representing circumferential turning angles between disk and rim. In the contribution, the diagnostic system is described and the measured data including damage analysis are presented.

Key words: *vibration, deformation, damage, railway wheels*

1. Introduction

The new vibrodiagnostic system VDS-UT2 designed for long-term monitoring of wheel vibration and wheel deformations under operation conditions has been developed [1], [2] and [3]. This system is applicable both for wheel development, e.g. improving reliability and decreasing noise of composed rubber-damped tram wheels, and for a diagnostic of dynamics and stability of a wheel and a wheel set on the track.

The development of the system including the development of sensors, wheel signal transmission, data storage and processing as well as telemetric data transfer via Internet connection for a remote control lasted three years. It involved elaboration of both the radiotelemetric system with the extensometer E-UT2 connected to the telemetric transmission unit RTM-UT2 and the contactless time-shift measuring system based on generating of impulses in consequence of magnetic field changes in a vicinity of a sensor. The new version of the equipment DIO designated for measurement, processing and storage of analog and digital signals has been developed in cooperation with the company Starmans Electronics, s.r.o., too. Measured digital data were transmitted in differential mode for higher resistivity to electrical disturbances. The vibrodiagnostic system has been completed by the remote control and remote measuring data logging via mobile phone net. The system was successfully applied on the wheel of the tram train KT8D5 of Municipal transport Brno. A few-weeks' measurement was being performed on the tram operating in standard passenger city line traffic. The measured values of axial, radial and circumferential displacements of the rim relative to the disk under different drive regimes were used for the evaluation of cycle counts

* Ing. L. Pešek, CSc., Ing. F. Vaněk, CSc., prof. Ing. M. Balda, DrSc., Ing. P. Procházka, CSc., Ing. P. Vaněk, J. Cibulka, Ing. V. Bula, Institute of Thermomechanics AS CR, v.v.i., Dolejškova 5, 182 00 Praha 8

of operating deformation of damping rubber segments moulded between the rim and the disk. Using fatigue life curves, the cycle counts for alternating and mean deformations were further utilized for the lifetime assessment of the rubber material.

2. Brief description of the vibrodiagnostic system

For the vibrodiagnostic system, in terms of a relative rim-disk motion measurement, two methods have been developed: a) the extensometer EX-UT2 with a strain-gauge displacement sensor and high-frequency signal transmission with radio-telemetric equipment RTM-UT2 and b) time difference method. A measurement unit continuously stores the output signals from both methods. The vibrodiagnostic system VDS-UT2 involves all these components.

The relative displacements are measured by beam deformation elements equipped with Si strain gauges in semi-bridge topology at the case of EX-UT2. The design of the RTM-UT2 for a signal transmission came out from the radio-telemetric equipment RTM-UT, developed previously in IT AS CR, v.v.i. and manufactured by a company JELEN. This system has been designed for parallel signal transmission from sensors placed on blade disks of turbines. The needed expansion of the origin measuring frequency range 20–8000 Hz of the former system to low frequencies of slowly alternating deformations, temperatures and accelerations was achieved by converting voltage changes to frequency ones. The carrying high-frequency electromagnetic waves transmitted from an aerial of the sensor are modulated by a measured sensed signal. An aerial placed on the bogie of the tram receives transmitted signals. Wireless transmitted high-frequency voltage is demodulated to low carrying frequency in the receiver. Voltage proportional to the strain-gauge signal is obtained after demodulation of the second carrying frequency. The miniature hybrid transmitter and receiver by company RADIOMETRIX with carrying frequencies 433 and 410 MHz approved by the Czech Telecommunication Institute operational measurements were used. The equipment for the second frequency modulation and demodulation was developed and built on integrated circuits (PLL). The radio-modem was completed by a loop aerial. The functional dependence of the output voltage on the relative displacement was determined by calibration with the opto-electronical positioning method using a PSD detector.

The contactless part of the vibrodiagnostic system is based on a time difference measurement of output impulses generated by two sensors placed on the stator. The sensors capture edges of the rim FZO and disk FZD phase marks. The marks made of thin steel sheet were distributed uniformly along the wheel circumference and joined to the wheel by welding. Signals of the two sensors are amplified and transformed to a symmetric output. They are conducted by a twisted pair of cables due to a high resistivity against disturbances. Additional phase mark and the sensor of phase mark FZ (MRFZ-UT) were installed in the similar way as the impulse phase marks and sensors on the wheel and stator for synchronization of the measurement channels under a wheel revolution.

The unit DIO 3000 with AD convertor (16 single-ended ± 10 V channels, resolution 12 bit) was developed in cooperation with the company Starman Electronics s.r.o. for the measurement and storage of analog and digital signals. Nine digital input channels with storage of internal counter state of events work parallel to the analog channels. Time resolution of the digital channels is 40ns. The sampling frequency of each analog input channel logging data into HD ranges up to 30 k words/s for 16 analogue channels and rises up to 150 k words/s in case of two channels. Data are transferred in packets via USB and they are saved in a binary code. The packets contain synchronization bits, time and active analogue channel data and digital channel data if an event has arisen.

The measuring and storage system DIO920B has been verified on the bases of parallel comparative measurement with the digital storage oscilloscope YOKOGAWA DL750 and numerical processing of the measured data by numerical programs developed in the MATLAB and TestPoint environment.

3. Operational deformation measurement on composed tramp wheel

The developed sensors and measurement system equipped with telemetric transmission for measurement of the composed wheels were tested in our laboratory before using in the operational conditions on tracks of a company DP Brno in November 2006 and May, August and November 2007.

The extensometers were installed on the right wheel of the leading wheel set of the tram KT8D5 in Central Works of DP Brno in Medlánky. The tram technical parameters are: length 30.3 m, width 2.5 m, height 3.145 m, mass 38 t, 231 people (54 seats and 177 stands), 8 wheel sets (each of them driven by an electromotor of 45 kW), max. speed 65 km/h. New wheels of the tram were installed for the trial operation in June 2006. The operational deformations of the wheel (⌀700 mm) were measured first on straight and loop tracks in the region of Stránská Skála (May 2007) and then on a track of the tramline number 1 (August and November 2007). During the first measurement the telemetric system of the company Jelen was used for a transmission of alternate dynamic loading. The innovated telemetric system RTM-UT2 extended for measurement of a static loading was used in the next case.

Three analog signals, i.e. axial AE or circumferential OE or radial RE deformations (channel 1), axial acceleration (channel 2) and longitudinal acceleration (channel 3), were recorded. Both accelerometers were fixed on the bottom gearbox cover in the wheel set middle. Accelerations were measured by two-axis feedback monochip accelerometers Motorola with a range 3g. The accelerometers suit for measurement on the wheel even though they undergo high overloading caused by centripetal acceleration and impact loading due to their advantageous size, mass, functionality and long-term stability. Sampling frequency of analog signals was set to 100 Hz. Eight-channel anti-alising filter of the third order with a cut-off frequency 30 Hz was manufactured for analyzing the frequency spectra up to 30 Hz.

Since the telemetric system RTM-UT2 was installed as one channel, the axial AE, circumferential OE and radial RE deformations were measured separately in period of October the 15th–18th, October the 19th–23rd and October the 24th, respectively.

The time instants of passages of the phase mark FZ, disk marks FZD and rim marks FZO were measured as digital signals and the times of rising or falling mark edges were recorded. Eight marks were distributed along the circumference of the rim and the disk. One phase mark was fixed on the other diameter than FZDs and FZOs (see Fig. 1). The mark FZ served for an identification of the FZDs and FZOs order number.

From time differences Δt_{ij} (mark number $i = 1, \ldots, 8$, revolution number $j = 1, \ldots, n$) evaluated from differences of trigger times of neighbouring mark FZD and FZO in particular revolutions we obtain relative circumferential displacement Δv_{ij}

$$\Delta v_{ij} = \Delta t_{ij}\, \dot{v}_{ij} = \Delta t_{ij}\, \omega_{ij}\, r = \Delta t_{ij}\, \pi\, f_{ij}\, d\ , \qquad (1)$$

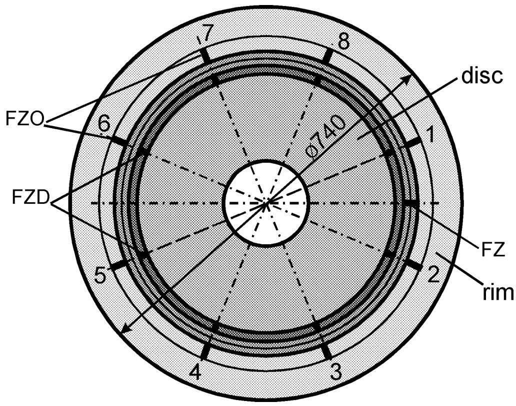

Fig.1: Scheme of a mark distribution for contactless circumferential displacement measurement

where ω_{ij} is an instantaneous rotational frequency (rad/s), f_{ij} is a revolution frequency (Hz), d is a diameter of circle on that the marks are distributed. Instantaneous frequency is evaluated from differences of trigger times of the disk marks for each revolution.

Since the differences Δv_{ij} are biased by systematic deviations due to a mounting inaccuracy of trigger mark edges (rising or falling) from the radials, the mean values $\Delta\bar{v}_i$ for each mark i and each revolution j were evaluated and subtracted from Δv_{ij}

$$\Delta\tilde{v}_{ij} = \Delta v_{ij} - \Delta\bar{v}_i \ . \qquad (2)$$

4. Results of deformation measurement of the wheel

The aim of the operational deformation measurement was to ascertain deformation ranges and time histories. Counts of closed cycles separated to classes according alternating (amplitude) and mean values in a measured deformation range (Rainflow matrix) were evaluated by the Rainflow algorithm. One-hour deformation records (see Fig. 2–4) were processed by this cyclic analysis. The one-hour period corresponds approximately the driving period of the tram from one end station to the other.

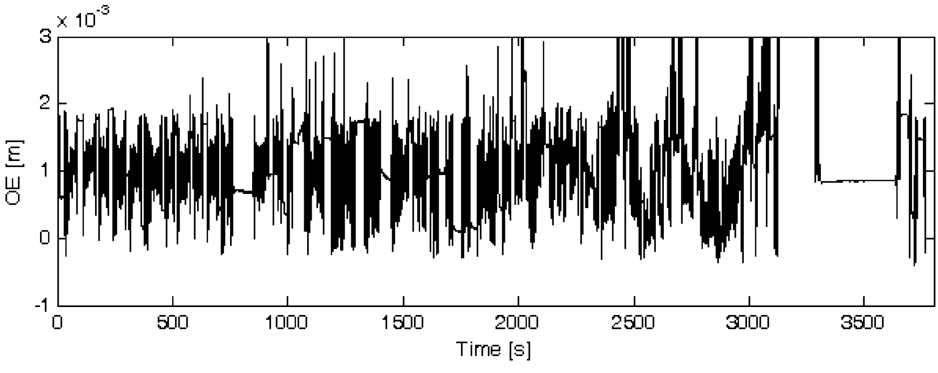

Fig.2: Circumferential deformation time characteristic

The circumferential deformation characteristic has a direct offset of app. 1 mm. The shift is caused by a spurious indentation in the measuring dural member that was created by contact forces between deformed and deforming members during operation. These members transferred relative displacements between the rim and disk.

Interesting finding is that the signal (Fig. 2) does not return to zero stationary value (1 mm) at the tram stops (time intervals without alternate components) but non-zero values in a range of ± 1 mm with respect to the zero stationary value appear. These values do not represent the permanent deformations of the segments but static restoring deformations that had arisen due to prestress by a braking or by a descent standing. In some cases, the prestress is accompanied by a flux process that causes an additional deformation with an exponential characteristic. This process is typical for viscous-elastic materials as rubbers.

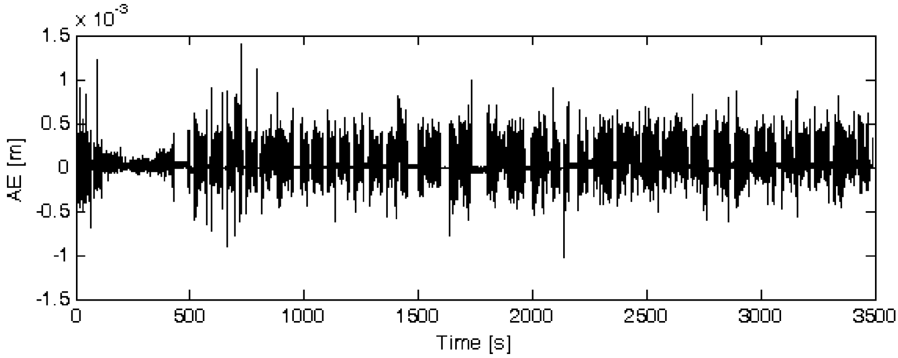

Fig.3: Axial deformation time characteristic

It is proven that the axial deformation (Fig. 3) is the least of all three measured deformations. It is a consequence of a high axial stiffness of the wheel. Time intervals with constant values correspond to tram stops and the maximum values correspond to the highest riding speed of the tram. Loading of the wheel is dependent on a position in the train. The measured wheel was still on the right side of the tram with respect to the riding direction. The deformation characteristic (Fig. 6) appears mainly in positive values.

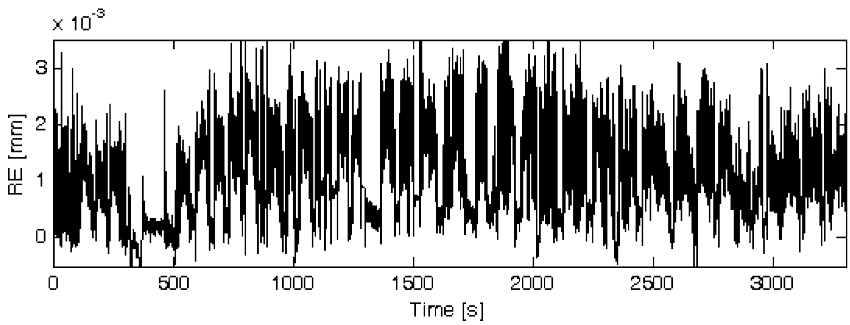

Fig.4: Radial deformation time characteristic

The asymmetry (app. 0.5 mm) of the radial deformation time characteristic to a horizontal axis is caused by a zero value setting at calibration. The deformations above this value mean compression and bellow this value decompression. Mass of passengers contributes to the additional deformation offset.

The decomposition of one-hour records of axial, circumferential and radial deformations to closed cycles by the Wavelet transform is depicted in Fig. 5. Amplitudes of dynamic radial deformations are in a range 0.2 to 0.4 mm. They are lower than static deformations since the dynamic stiffness is greater than static stiffness. The offset 0.5 mm is caused by the above-mentioned setting of zero value.

For circumferential deformation, besides cycles with zero mean deformation, a group of cycles with mean deformation around 0.7 mm and -0.5 mm can be observed. These mean deformations are caused by braking and starting drive regimes. This group is more distinct for breaking.

Circumferential deformations evaluated by the contactless time interval method and by extensometer analog measurement can be compared in the Fig. 6.

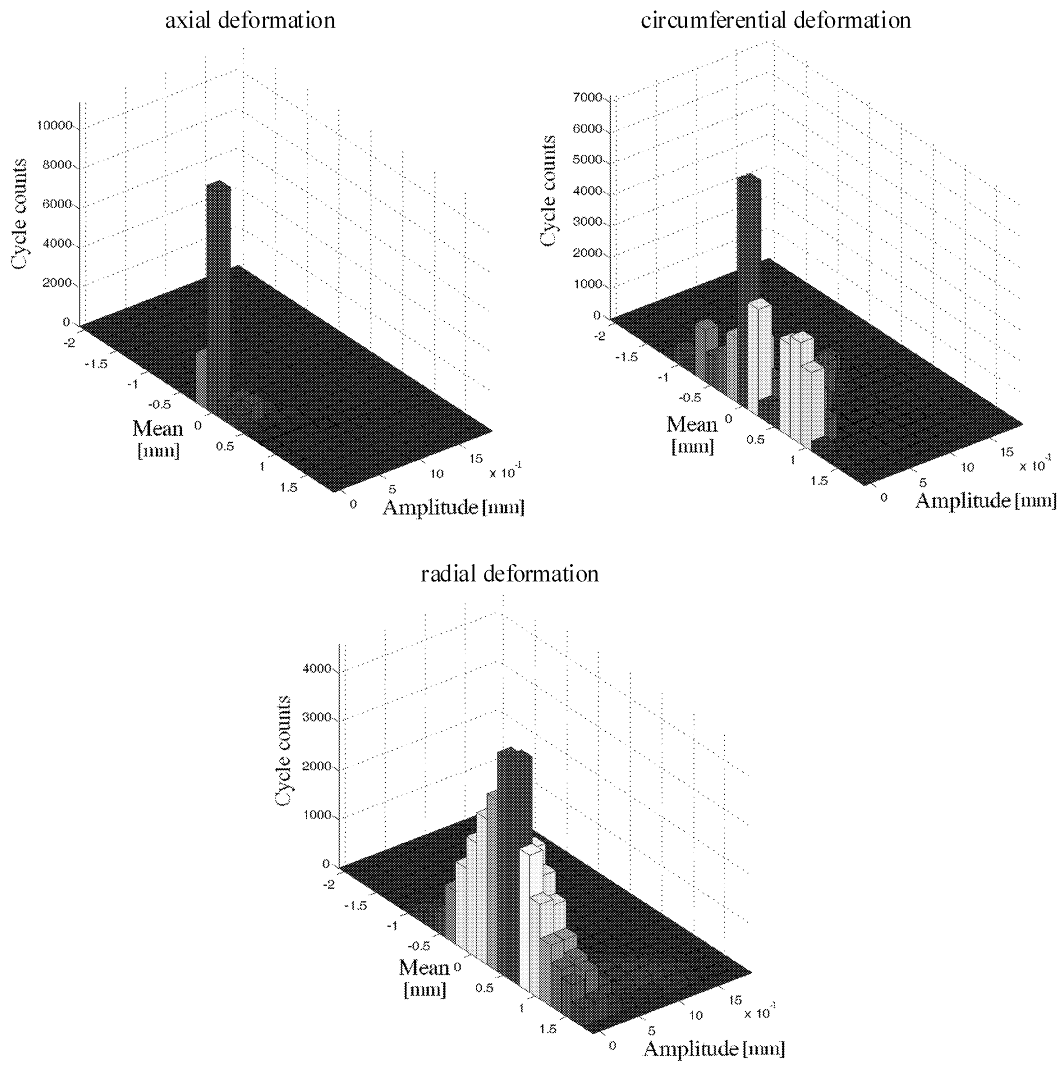

Fig.5: One-hour Rainflow matrices of axial, circumferential and radial wheel rim-disk deformations – October 2007

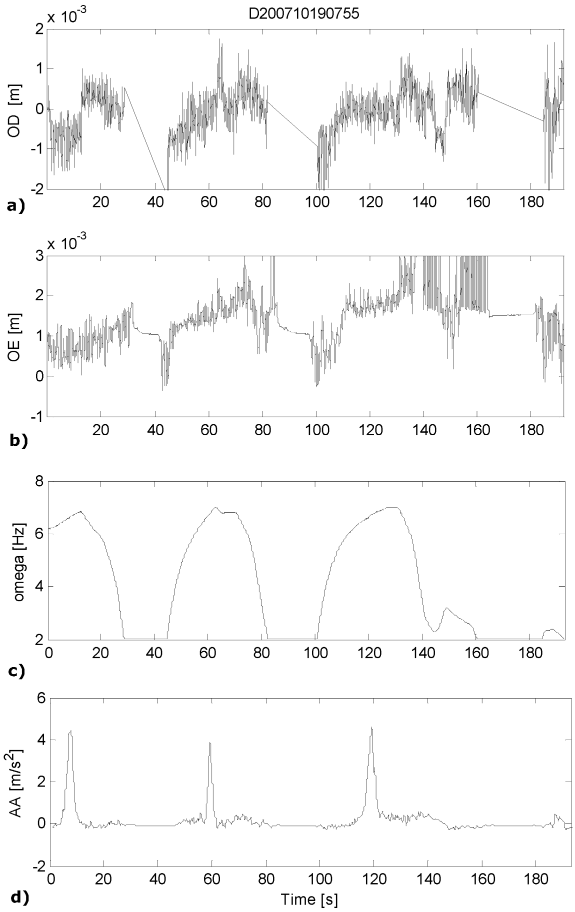

Fig.6: Circumferential deformation characteristics from a) time interval method, b) extensometer measurement; revolution wheel frequency c) and axial wheel set acceleration d) are depicted, too

The analog measurement of the circumferential deformation OE (Fig. 6b) was modified by a moving average algorithm over ten samples for noise suppression. Evaluation of OD dependence (6a) was performed by the previously described method. The same time character of the signals OE and OD is obvious from the characteristics 6a, b. The signals are shifted one to another by the steady value 1 mm as mentioned above. Higher level of noise is visible at the dependence OD. The regimes with revolution frequency below 2 Hz were not evaluated (see 6c) due to an elimination of transient driving regimes from the OD dependence evolution. The direct lines in the dependence OD fill time spaces between measured intervals. Deformations extend in a range app. $\langle -2, 2\rangle$ mm. Increase of the deformation at the starts and a decrease at the breakings is visible. The deformation represents a relative movement between rim and disk. Considering the rim a reference (standstill system), the deformation increase (positive increment) represents revolution of the disk in a riding revolution direction and the decrease (negative increment) means revolution against the ride direction.

An example of permanent deviations $\Delta\bar{v}_i$ $(i = 1, 2, \ldots, 8)$ of the triggering mark edges is depicted in Fig. 7. Rising edges of the disk marks and falling edges of the rim marks were recorded in this case. Changes in a direct value indicate the mutual revolution of the disk

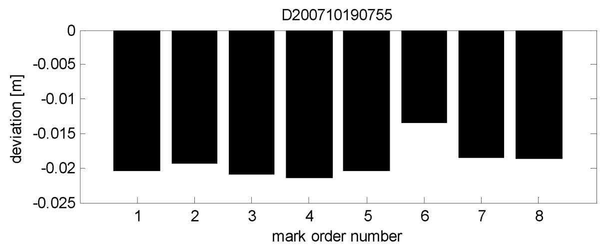

Fig.7: Permanent deviations of triggering mark edges at a measurement of circumferential deformation by the time difference method

and the rim. Therefore, this change can serve as a diagnostic parameter of slewing caused by a lowered rim-disk coupling to torque. Rubber segments transmit the coupling.

Dynamic responses of the wheel on straight and bow tracks were measured on the tramline Stránská Skála – Medlánky in 2006. Riding path of the tram was recorded by navigation GPS Receiver PR-355. The measured time responses were used for next processing to Rainflow matrices and spectrograms of axial, radial and circumferential deformations. The spectrograms (scale in dB) and Rainflow matrices of all three deformations are in Fig. 8, 10 and 12 are in Fig. 9, 11 and 13, respectively, for case of straight track at speeds 20 and 40 km/h. The direct components of analog signals were not measured in this case.

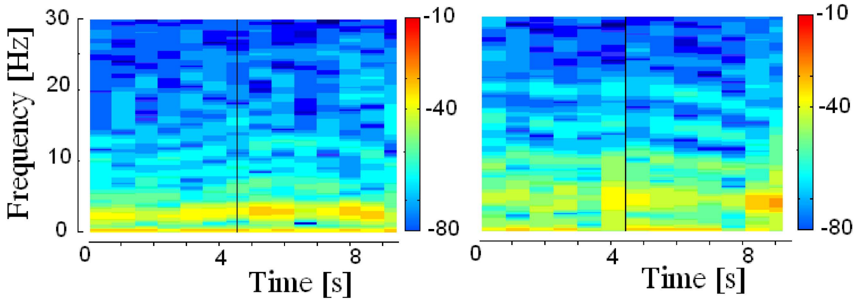

Fig.8: Spectrograms of axial deformation AE – direct track 20, 40 km/h ($u_{\mathrm{ref}} = 1$ mm)

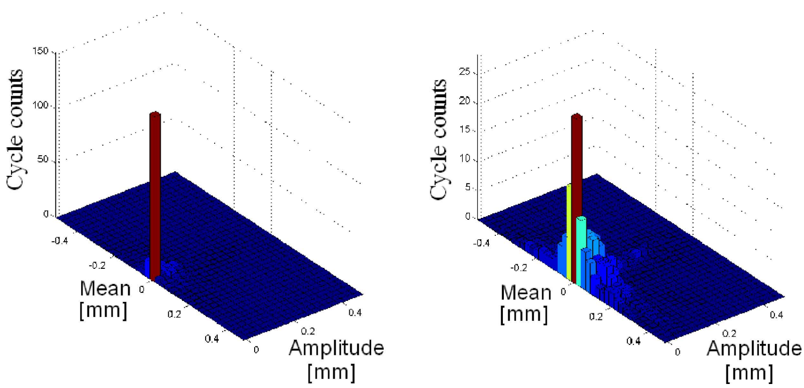

Fig.9: Rainflow matrices of axial deformation AE – direct track 20, 40 km/h ($u_{\mathrm{ref}} = 1$ mm)

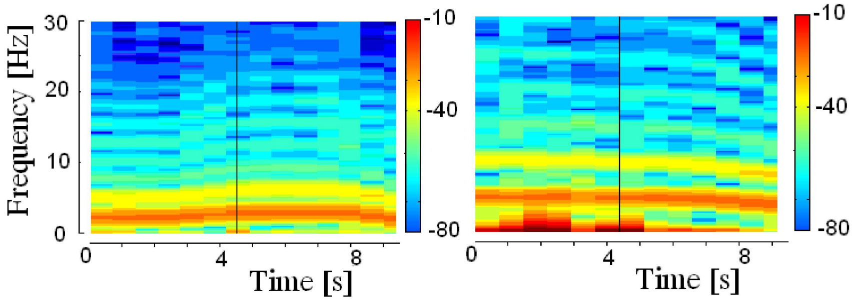

Fig.10: Spectrograms of radial deformation RE – direct track 20, 40 km/h ($w_{\mathrm{ref}} = 1$ mm)

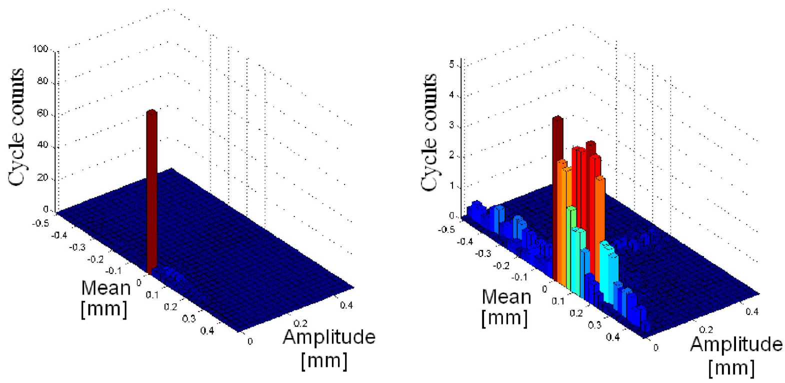

Fig.11: Rainflow matrices of radial deformation RE – direct track 20, 40 km/h

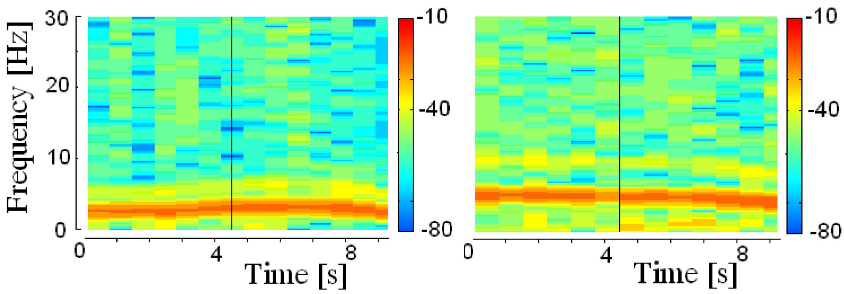

Fig.12: Spectrograms of circumferential deformation OE (Radiometrix) – direct track 20, 40 km/h ($v_{\mathrm{ref}} = 1$ mm)

Dominant branches (highest amplitudes) corresponding to a frequency of revolution are clearly detectable from all deformation spectrograms. There are also visible the second and third harmonics of the revolution frequency on radial and circumferential deformations. Their dependence on the revolution frequency is caused by rubber deformation changes due to a carriage mass during a wheel turning. The maximum (compression) and minimum (decompression) values can be observed in positions 6 and 12 o'clock, respectively, and zero values in positions 3 and 9 o'clock for the radial deformation. It is different for the circumference deformations. Maxima occur at 6 and 12 o'clock positions and zeros at 3 and 9 o'clock positions. These cyclic changes of axial deformations can be evoked by a wheel shimmy in axial direction.

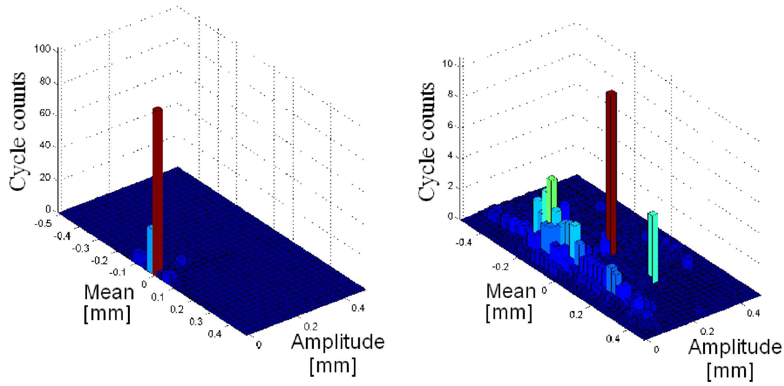

Fig.13: Rainflow matrices of circumferential deformation OE – direct track 20, 40 km/h

Resulting Rainflow matrices for different speeds were obtained by averaging of several rides for each track profile (straight and bow). The cycles of particular ride were first classified according to mean value and alternating value and then averaged together according to the classes. The matrices show an increase of alternating (amplitude) values with a speed increase.

5. Estimation of residual life-time of rubber segments

Laboratory tests were performed for an estimation of a rubber segment lifetime [4], [5]. Static and dynamic rubber characteristics were ascertained in a temperature range −10 to −50 °C with evaluation of a cyclic loading influence. Lifetime curves of the rubber segment at temperatures 20, 0, −20 and −40 °C were evaluated. Influence of low temperatures on friction behaviour of rubber was examined under shear tests with a steel band pressed-in by rubber blocks. Withdrawal of the steel band out of a central position under cyclic loading was measured.

The force needed for a designed amplitude level increases with a decrease of temperature as was found out from static characteristics. In the temperature range $0 \div -35$ °C, the force increase is negligible. Higher force increase begins under lower temperatures than −40 °C, when rubber gets stiff and force rapidly grows. The recovery process starts and deformation decreases after the unloading and withdrawal of the segment from a climatic chamber. However, the stiffening remains in a material memory and new quasi- static hysteresis loops (10 mm/min) differ from the loops in a virgin material state (the 4^{th} loop considered for elimination of Mullin's effect). Force-deformation hysteresis loops were measured at an amplitude $P_{\text{a}} = 3$ kN, prestress $P_{\text{m}} = -5$ kN and frequency $f = 2$ Hz after 150, 5000, 10000, 20000, 50000 and 75000 cycles. The results showed that the amplitudes of segment vibration decrease with a decrease of temperature and stiffness increases at the same time. This effect is substantial at origin up to 5000 cycles but it decreases with an increasing number of cycles. The rubber segment stops getting stiffer but a permanent deformation is growing.

It has been proven that a cyclic deformation influences material behaviour especially at lower temperatures. Even after a long time of recovery the sample deformation does not get to an origin state and it is accompanied by a change of static characteristic. Therefore, the aim was to ascertain after how many cycles of dynamic loading the rubber segment achieves 10 % of permanent deformation. This 10 % of deformation was evaluated directly after the unloading and at the adjusted temperature without a recovery time. The size of the permanent deformation is dependent on not only a number of cycles but also on a level of static prestress and temperature. The test were carried out for temperatures 0 °C, −20 °C a −40 °C and a room temperature [4] and for two static prestresses $F_\mathrm{m} = -5$ and -8 kN. Lifetime curves presented here were ascertained for a room temperature (Fig. 14).

The effect of low temperatures on a rubber lifetime can by described as the lower temperature the higher number of cycles N at a lower value of prestress $F_\mathrm{m} = -5$ kN. However at higher prestresses $F_\mathrm{m} = -8$ kN the cycle number rapidly decreases and a damage progresses rapidly. It is valid especially for temperatures lower than −35 °C and −45 °C, when the mechanical behaviour starts to change (glassy transition). Regression lines describing lifetime curves and Haigh diagrams were analytically constructed based on the experiments. The Haigh diagram describes a dependence of critical loading amplitude F_a normalized by a fatigue limit F_c and a static prestress F_m.

The evaluation of material damage coming out of operational loading has not been fully solved even for current construction materials by now. The reason is the insufficient knowledge of physics of damage of material under generally varying strain in size and direction. Furthermore, rubber-like materials change under long-term loading due to creeping, temperature dependence, crystallization process, and atmospheric influences. Some changes are reversible due to a material recovery and some irreversible and cumulate according to history of mechanical and temperature loadings and environmental conditions. In addition, the isoprene rubber that was used for segment production suffers an aging (stiffening) by oxygenation for temperatures above 70 °C.

We used well-known Palmgren-Miner hypothesis [6], which was applied on closed cycles obtained from a decomposition of time variable loading process (Fig. 4), for the first approximation of a damage assessment. Lifetime curve (Fig. 14) and Haigh diagram (Fig. 15) were used as input material parameters for description of damage. The damage matrix of relative damages of the segment was calculated (Fig. 16) using Rainflow matrix. Material constants were chosen: dynamic stiffness 3.5 kN/m; conventional fatigue limit $F_\mathrm{c} = 0.2$ kN was chosen for a limit cycle number $N_\mathrm{c} = 1{\times}10^8$; exponent of Wöhler curve $w = 2.4333$; coefficient of Haigh diagram $k_\mathrm{H} = 0.8$; fictive critical force in Haigh diagram $s_\mathrm{F} = 20$ kN. Since we had only fatigue tests with a static compression and pressure pulsations the damage evaluation was ascertained just from operational radial deformations. Combination of pressure and shear straining occurs in praxis due to a geometrical slope of the segment to radial axis (app. 15°) a c. However, the shear straining was not considered here.

It is necessary to emphasize that the quantitative information is not solid but a conventional one, since on the contrary to metals, the critical values as fatigue limit F_c and strength limit R_m are not measurable for rubber-like materials. They were estimated in this work as limit values with respect to the reliability of the compliant transmission inside the wheel.

From the damage matrix, it is obvious that the highest damages are caused by deformation classes of higher amplitudes. The relatively high degree of damage is probably caused by a non-fully valid assumption of linear damage cumulation by a cyclic loading. The rubber damage seems to be overestimated for the thermo-viscous-elastic materials and the chosen reliability criteria.

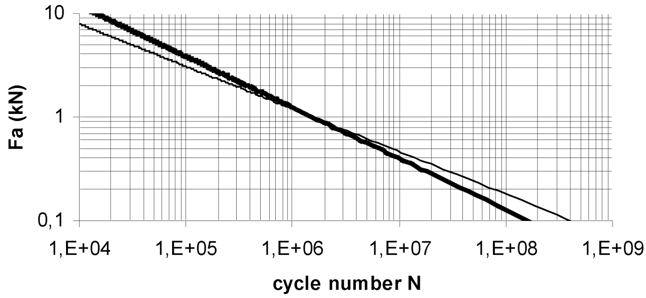

Fig.14: Lifetime curves of rubber segments at temperature 20 °C (thin line −5 kN, thick line −8 kN)

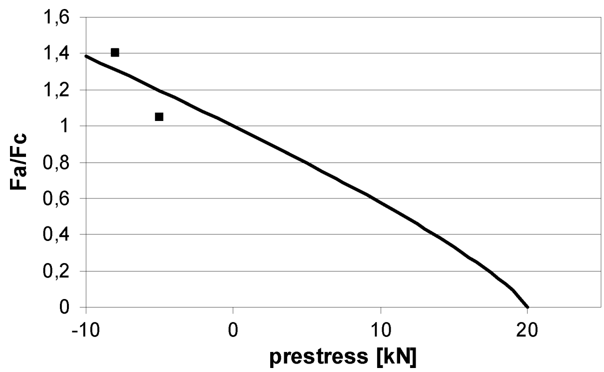

Fig.15: Haigh diagram (F_a critical loading amplitude, F_m static prestress, $F_c = 0.2$ kN fatigue limit); filled quads – measured values

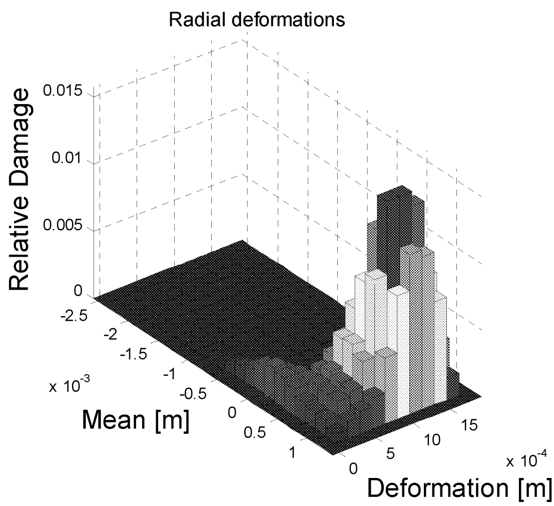

Fig.16: Damage matrix of the rubber segment for radial loading

6. Conclusion

The vibrodiagnostic equipment VDS-UT2 with a remote communication via Internet connection for a long-term monitoring of vibration and static and dynamic deformations of railway wheels under operation has been designed and developed during the last three years. The sensor Extensometer UT2 with telemetric transfer having double frequency modulation features an accuracy of app. 0.03 mm. The contactless sensor for time and amplitude difference measurement by impulse method based on magnetic field changes is aimed at long-term rubber segment deformation measurement. However, for setting to continuous duty the analog circuits should be better encapsulated against the severe operational conditions (temperatures, humidity and electrical disturbances). The contactless system demands improving of sensors fixing to the wheel set bearing case as well.

Experimental research of reliability of rubber segments with evaluation of static and dynamic characteristics has run over plus and minus temperature ranges. Furthermore, the fatigue tests at pressure loadings that lead to curves of lifetime evaluation have been performed. The evaluation of friction force dependences on amplitudes and adherence pressure sizes have been elaborated. As the first approximation of damage assessment of rubber segments Palmgren-Miner hypotheses of cumulative damage from the closed cycles of service loading were used. The quantitative information presented here is not solid but conventional, since the critical material values for fatigue analysis are not measurable for rubber. They were estimated as limit values with respect to the reliability criteria proposed for the compliant component of the wheel.

The model of a damage and permanent deformation evolution at dynamic long-term loading has not been fully analytically described due to time variant behaviour of rubber by now. It is evident from our experimental research that for analyzed isoprene rubber a lifetime increases with an increase of mounting prestress by plus temperatures and that it decreases by minus temperatures. The stiffness grows and the amplitude of deformation falls down from the operation force loading both due to minus temperatures and prestress increase. We consider desirable for lifetime optimalization to complete achieved lifetime curves also for higher values of prestress and for modified reliability criterion to 10 % of a permanent deformation evaluated after a recovery period. Furthermore, the number of test cycles should be raised up to 10^7 at least. Repeated operational measurements with suppressing of spurious influences, especially electrical, to get a more accurate damage assessment and a direct measurement of deformations on the rubber segment are advisable, too.

Acknoledgement

This work has been solved in a frame of the grant project GA CR No. 101/05/2669 'Dynamics and reliability of vibrodamping elements of termo-viscous-elastic materials'.

References

[1] Pešek Luděk - Veselý, Jan - Vaněk, František - Cibulka, Jan - Bula, Vítězslav: Návrh, vývoj a realizace měření vibrací jedoucího tramvajového kola bez a s přídavným tlumičem, Výzkumná zpráva Z1391/06, Praha, ÚT AV ČR, 2006, 42 s.

[2] Pešek L., Vaněk F., Cibulka J., Hendrych P.: Vibration and noise of railway tram wheels on track, McMAT 2007, ASME Conference, Austin : University of Texas, Austin, (2007), S. 1–1

[3] Pešek L., Vaněk F., Veselý J., Cibulka J., Boháč T.: Measurement of vibration and noise of railway wheels on track, Proceedings of ISMA2006 Leuven, Heverlee : Katholieke Universiteit Leuven, 2006 – (Sas, P.), p. 4395–4407

[4] Svoboda J., Pešek L., Fröhlich V.: Vlastnosti termo-visko-elastického materiálu 42-809 pro výrobu vibrotlumících prvků – 3. část, Výzkumná zpráva Z-1406/07 ÚT AVČR, v.v.i., 2007

[5] Svoboda J., Pešek L., Fröhlich V.: Experimental study of termo-visco-elastic material behavior at low temperatures, Applied and Computational Mechanics, Volume 1, Number 1, 2007, ISSN 1802-680X
[6] Balda M., Svoboda J., Fröhlich J.: Odhadování únavové životnosti části při kombinovaném náhodném zatěžování, Inženýrská MECHANIKA, roč. 10, 2003, č. 5

Received in editor's office: March 25, 2008
Approved for publishing: June 200, 2008